

Harvesting Roadway Solar Energy-Performance of the Installed Infrastructure Integrated PV Bike Path

Shekhar, Aditya; Kumaravel, Vinod Kumar; Klerks, Stan; de Wit, Sten; Prasanth, Venugopal; Narayan, Nishant; Bauer, Pavol; Isabella, Olindo; Zeman, Miro

DOI

[10.1109/JPHOTOV.2018.2820998](https://doi.org/10.1109/JPHOTOV.2018.2820998)

Publication date

2018

Document Version

Final published version

Published in

IEEE Journal of Photovoltaics

Citation (APA)

Shekhar, A., Kumaravel, V. K., Klerks, S., de Wit, S., Prasanth, V., Narayan, N., Bauer, P., Isabella, O., & Zeman, M. (2018). Harvesting Roadway Solar Energy-Performance of the Installed Infrastructure Integrated PV Bike Path. *IEEE Journal of Photovoltaics*, 8(4), 1066-1073.
<https://doi.org/10.1109/JPHOTOV.2018.2820998>

Important note

To cite this publication, please use the final published version (if applicable).
Please check the document version above.

Copyright

Other than for strictly personal use, it is not permitted to download, forward or distribute the text or part of it, without the consent of the author(s) and/or copyright holder(s), unless the work is under an open content license such as Creative Commons.

Takedown policy

Please contact us and provide details if you believe this document breaches copyrights.
We will remove access to the work immediately and investigate your claim.




Green Open Access added to TU Delft Institutional Repository

'You share, we take care!' – Taverne project

<https://www.openaccess.nl/en/you-share-we-take-care>

Otherwise as indicated in the copyright section: the publisher is the copyright holder of this work and the author uses the Dutch legislation to make this work public.

Harvesting Roadway Solar Energy—Performance of the Installed Infrastructure Integrated PV Bike Path

Aditya Shekhar , Vinod Kumar Kumaravel, Stan Klerks, Sten de Wit, Prasanth Venugopal, Nishant Narayan , Pavol Bauer , Olindo Isabella, and Miro Zeman

Abstract—Solar road technology provides an opportunity to harvest the vast, albeit dispersed, photovoltaic (PV) energy, while maximizing the land utilization. Deriving experience from the pioneering 70-m solar bike path installed in the Netherlands, this paper highlights the operational challenges and performance parameters using the first-year measured data. The theoretically predicted energy yield is compared with the measured energy yield. Based on the best performing module, the benchmark annual energy yield is set to 85–90 kWh/m² specific to the installation site. It is shown that this value can be bettered by about 1.5 times if different cell technology such as monocrystalline is used. With different installation sites around the world, thermal behavior as well as annual energy yield changes. Theoretical proof is offered that it is not unreasonable to expect an annual energy yield in the upwards of 150 kWh/m² with solar road energy harvesting technology. For example, the annual yield is found to be 213 kWh/m² if the same model is simulated for a solar road PV installation in India, which increased further with the use of monocrystalline to almost 300 kWh/m².

Index Terms—Annual energy yield, energy harvester, infrastructure integrated photovoltaics (IIPV), module temperature, photovoltaics (PV), roadway, solar pavement, solar powered street, solar road (SR).

I. INTRODUCTION

RESEARCHERS are increasingly looking toward the sun for sustainably meeting the energy needs of the human civilization. Recent years have seen rapidly decreasing costs of solar photovoltaic (PV) modules at growing operating efficiency. It was reported that for every doubling of module shipments in terms of MWp, the selling prices have decreased by 22.5% [1], while experimental demonstrations show that cell efficiency in the upwards of 20% is achievable [2], [3].

Manuscript received January 6, 2018; revised March 3, 2018; accepted March 22, 2018. Date of publication April 16, 2018; date of current version June 19, 2018. (Aditya Shekhar and Vinod Kumar Kumaravel have contributed equally to this paper.) (Corresponding author: Aditya Shekhar.)

A. Shekhar, N. Narayan, P. Bauer, O. Isabella, and M. Zeman are with the Delft University of Technology, 2628 CD Delft, The Netherlands (e-mail: a.shekhar@tudelft.nl; n.s.narayan@tudelft.nl; P.Bauer@tudelft.nl; o.isabella@tudelft.nl; m.zeman@tudelft.nl).

V. K. Kumaravel is with Sungevity International, 1021 KP Amsterdam, The Netherlands (e-mail: vinodk.kumaravel@gmail.com).

S. Klerks and S. de Wit are with the Netherlands Organisation for Applied Scientific Research, 2595 DA The Hague, The Netherlands (e-mail: stan.klerks@tno.nl; sten.dewit@tno.nl).

P. Venugopal is with Qualcomm Halo, 81829 Munich, Germany (e-mail: V.Prasanth@tudelft.nl).

Color versions of one or more of the figures in this paper are available online at <http://ieeexplore.ieee.org>.

Digital Object Identifier 10.1109/JPHOTOV.2018.2820998

However, the ability to generate useful energy from solar irradiation is limited by the land constraint due to its dispersed nature. By harvesting the incident solar energy from roadways, it is possible to maximize the utilization of land dedicated toward transportation [4], [5]. Specifically, by using infrastructure integrated PV (IIPV) technology for powering the roadway loads, the grid dependence can be minimized, while also reducing the distribution losses and requirements for copper, thus providing economic benefits [6], [7]. IIPV may also contribute in mitigating issues related to significant infrastructure upgradation in distribution grids due to high forecasted demand with the advent of electric vehicles (EVs) [8]. A vision of sustainable highways integrating high-powered solar road (SR) PV generation, wireless power transmission to EVs, and self-healing asphalt for developing a seamless transportation electrification technology is presented in [9] and [10].

A. Roadway Energy Harvesting Technologies

Several technologies that can be used to harvest thermal and electrical energy from roadways are discussed in this section. With a focus on transporting water to islanded locations using bridge road links, especially designed pipes were embedded 125–175 mm below the road surface [11]. It was claimed that cost savings were achieved in water transportation, and in addition, the annual energy yield of about 770 kWh was obtained for every 6 m² of road surface by use of solar thermal collection. Cautioning that knowledge is required on effect of asphalt road-embedded pipes from the standpoint design, construction, and maintenance [5], the potential of extracting heat from asphalt pavement in positively influencing the roadway lifetime and regulating the urban heat island effect was highlighted in [12] and [13].

Using a piezoelectric transducer to convert mechanical strain from passing vehicles, energy can be harvested in electrical form [14], [15]. In [14], identifying interstate highways with high speed and traffic volumes as ideal candidates, the prototype with 4× piezoelectric elements was estimated to generate 1080 Wh per year based on the assumed traffic conditions. However, low power densities of ≈2 mW limited the application to off-grid LED traffic lighting and embedded wireless sensors. Combining this technology with communication methods, a novel “smart street” solution for detecting presence, direction, and speed of vehicles was developed in [16]. Extending the concept, energy savings may be achieved by design of



Fig. 1. Photo of the installed SR bike path. (For more information, see [25]).

intelligent lighting systems operating based on sensed vehicle movement [17].

The economic viability of the dedicated road-side solar-powered LED lighting system was studied in [6]. As compared with a grid-connected system, the solar-powered system had 13% lower power consumption but 37% higher installation cost. The main reason for higher costs was that of the PV module at 5 USD/Wp. With lowering module costs below 1 USD/Wp, as presented in [1], the payback can now be expected to be much lower. Interesting studies on solar-powered road-side units for applications such as traffic signals and road surveillance are carried out in [18]–[21].

The above roadway energy harvesting techniques are dominated by either thermal or low-powered electrical conversion capable of *in situ* consumption and environment regulation. High electrical power needs are driven by the advent of EVs and sustainable electrification of public transport systems [8], [22]. Implementation of solar PV plants for generating power with reasonable energy density for supporting the grid would require significant quantities of land, a need that inevitably competes with other important uses such as agriculture, housing, and transportation.

Even though the potential of SR-based IIPV generation is recognized [5], [23], [24], limited literature is available on the operational know-how of this technology in actual installation conditions. The object of this paper is to share the experience gained from the collected performance parameters of the installed SR IIPV bike path in The Netherlands after one operational year.

B. Installed Solar Road Infrastructure Integrated Photovoltaic Bike Path in The Netherlands

The SR bike path installed at Krommenie, the province of North Holland, is shown in Fig. 1.

The green cabinet toward the right of the image houses the grid-connected inverters. All relevant computations offered in this paper are corresponding to the location coordinates 52.494° N, 4.7666° E. Furthermore, the influence of static shading is incorporated in the model by means of horizon images taken at the location. In this respect, the SR can be subdivided into three zones covering a third of the road each. Horizon images indicated the maximum impact of static shading in Zone 3.

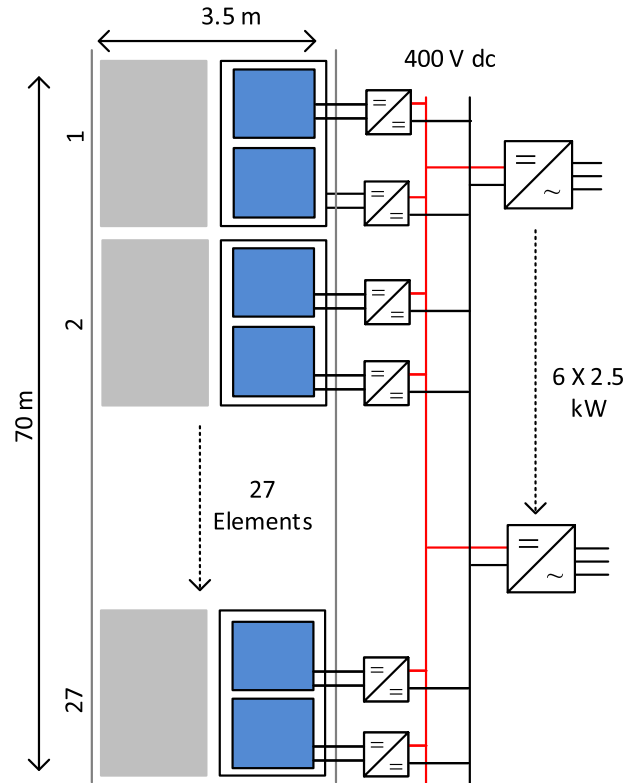


Fig. 2. Geometrical and electrical layout of the installed SR bike path.

II. SYSTEM DESCRIPTION

The SR bike lane consists of 27 precast concrete elements, of which one half is equipped with solar modules and the other half is a conventional concrete surface. Each of these elements have two modules, making a sum of 54 modules. These polycrystalline silicon modules are endowed with 80 wafer-based cells and exhibit a rated output varying between 293 and 313 Wp.

The schematic overview of the electrical system is shown in Fig. 2. The total dc power produced by all the SR modules is fed into six parallel-operating grid-connected inverters through the module-level dc/dc converter.

If the predicted dc power is greater than multiples of individual inverter rating of 2.5 kW, the SR power output is redistributed using an additional inverter. The theoretical energy yield estimates provided in this paper include the input-power-dependent efficiency curve of the 6× inverter system. Based on theoretical estimations, it was found that the inverter performance is close to its rated efficiency of 96% when the dc power produced by the SR (total for all modules) is higher than 1 kW. The peak predicted inverter power output was 10.5 kW.

III. THEORETICAL PERFORMANCE ANALYSIS

A. Global Irradiance at Installation Location

Corresponding to the azimuth and altitude of the sun for the location, the theoretical incoming irradiance in terms of both direct and diffuse components (W/m^2) is calculated for every minute of the year 2015 [26], [27].

The direct irradiance varies based on different cloud cover and rainfall and can be represented by the Linke turbidity factor

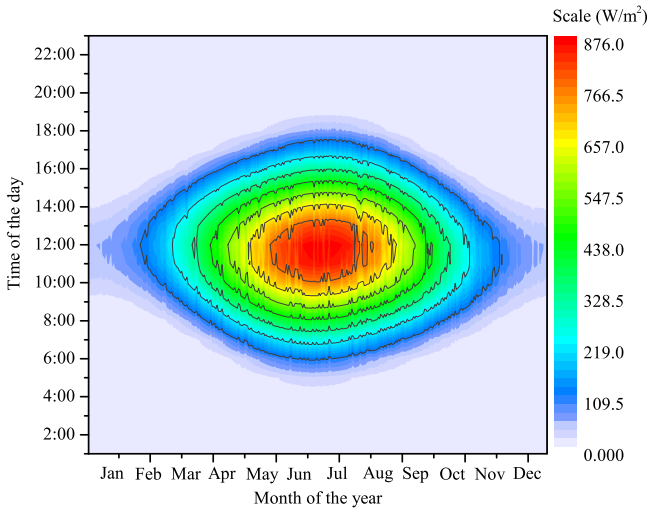


Fig. 3. Theoretically computed horizon-free global horizontal irradiance for the year 2015 at Krommenie.

(T_L). Some information with description on this factor at AM 2 is provided in [26]. T_L was incorporated in the corrected model by using the duration of rainfall (R_D) for varying the turbidity factor in four intervals given by

$$T_L = \begin{cases} 3.5, & \text{if } 0 < R_D \leq 10 \\ 4, & \text{if } 10 < R_D \leq 20 \\ 5.5, & \text{if } 20 < R_D \leq 30 \\ 6.5, & \text{otherwise.} \end{cases} \quad (1)$$

The diffuse irradiance is dependent on the diffuse angular function and the diffuse transmittance function, and these parameters are dependent on the altitude of sun. For more details on developing the irradiance model, see [28] and [29]. Fig. 3. shows the contour plot of theoretically computed global horizontal irradiance incorporating both direct and diffused components for Krommenie in the year 2015. The results were validated using the KNMI database for this location.

It can be observed that the irradiance is maximum between 10:00 A.M. to 2:00 P.M. throughout the year. Prominent disruptions in the contour lines during the months of July and August are due to higher turbidity factor in relation to (1). The maximum incident global irradiance is 876 W/m². The horizon-free insolation received by the SR for the year 2015 is 1038.8 kWh/m² with average sun hours of 2.84 per day.

B. Shading

The theoretically computed global irradiance is subject to static and dynamic shading. The Meteonorm software is used to determine the influence of static shading due to surrounding structures and trees. The SR pathway was divided into three zones of nine elements each. An image of the horizon was taken for each zone, and the mean of the sun hours experienced was computed to be 2.81, that is, a 1% reduction in irradiance due to static shading. The impact of dynamic shading due to the movement of bikes and surface dirt accumulation was not included in the theoretical model, which is, therefore, a contributing factor

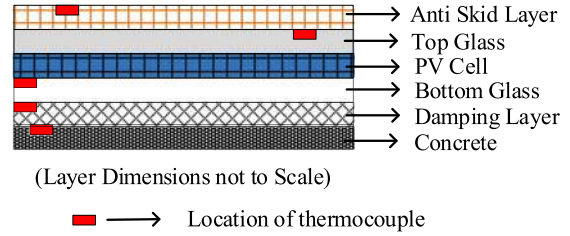


Fig. 4. Component layers of an SR element.

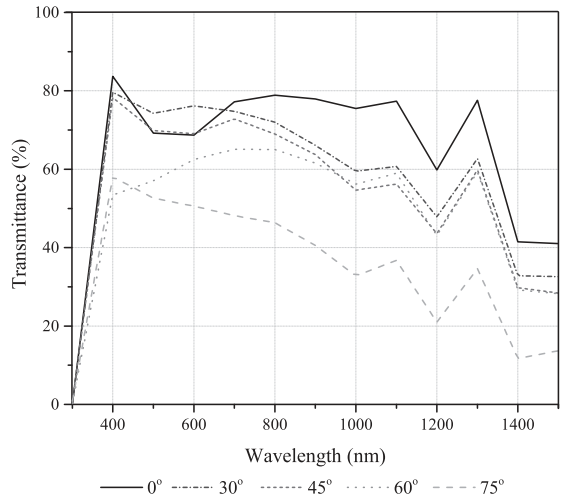


Fig. 5. Transmittance of light through the antiskid layer as a function of wavelength at different angles of incidence.

for deviation of this model in comparison with the measured data presented in this paper.

C. Transmittance Characteristics of the Antiskid Layer

The structure of an SR element is shown in Fig. 4. Individual layers and the location of thermocouples for temperature measurements are depicted.

The antiskid layer is installed at the topmost surface of the SR to provide adequate friction to the above moving wheels. This layer is not present in conventional rooftop PVs, and therefore, its optical properties influence the thermal and electrical performance of the SR. The transmittance of light through the antiskid layer was measured using the PerkinElmer Lambda 950 Spectrophotometer and estimated by following the mathematical approach described in [31], as shown in Fig. 5.

From our measurements and subsequent estimations based on [31], it was concluded that the antiskid layer is isotropic, with average spectral transmission decreasing from 73% to 45%, as the angle of incidence increased from 0° to 75°.

D. Thermal Behavior of a Solar Road Element

Since the PV modules are sandwiched between the antiskid layer on the top and the concrete slab at the bottom, the thermal behavior is different than conventionally installed modules. The additional antiskid layer on top alters the fraction of irradiance reaching the cell and, therefore, affects the temperature of the module.

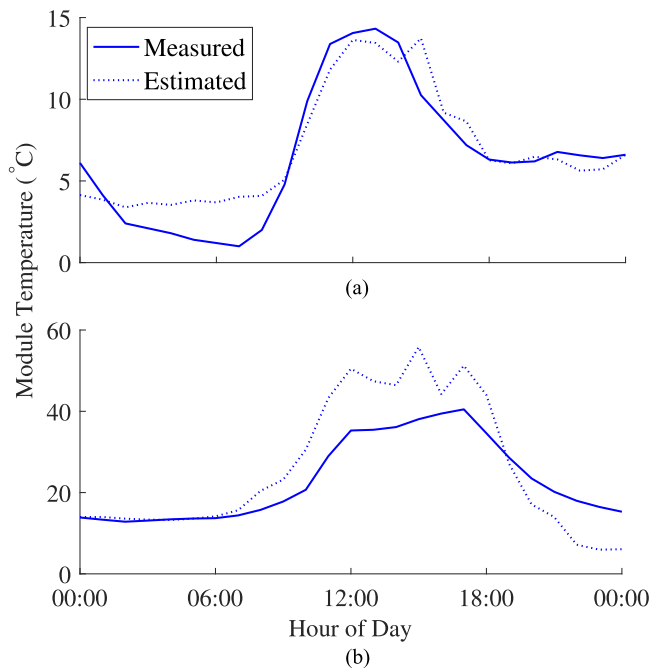


Fig. 6. Measured and estimated module temperatures. (a) Typical day in January. (b) Typical day in June.

As the PV module is installed below the ground surface, there is no convective cooling on its rear surface and reduced on the top surface due to the antiskid layer. Furthermore, the ground acts as a massive heat sink through the underlying concrete slab. The development of a detailed thermal model was deemed necessary not only to ensure that the SR element was operating within the thermal limits, but also to estimate the electrical performance deterioration due to the rise in operating temperature.

The principle of energy balance is used to estimate the 1-D heat transfer along the depth of the SR element [29]. Since the thermal time constant is about 7 min, the temperature of the module is determined every 10 min at the steady state [30]. Therefore, the thermal capacitance of the SR components is neglected. Considering the entire SR element as one block, a preliminary estimate is presented in a previous work by the authors [27]. The key difference in the temperature results shown in the present work is that the 1-D heat flow energy balance equations are applied for each layer of the SR shown in Fig. 4, represented by their thermal resistances. Furthermore, the measured optical properties of the antiskid layer discussed in the preceding section are used. The estimated module temperature is directly proportional to the irradiance with a maximum of 63.60 °C at about 1000 W/m². A comparison of the estimated and measured module temperatures for a typical winter and summer day is shown in Fig. 6.

It can be observed that the peak estimated temperature is lower than that measured in the month of January, when typically low peak irradiance and ambient temperature is expected. In June, on the other hand, the peak of the estimated temperature is significantly higher than the measured value. During this month, a high irradiance and ambient temperature is expected. This mismatch is expected due to several factors. Among them,

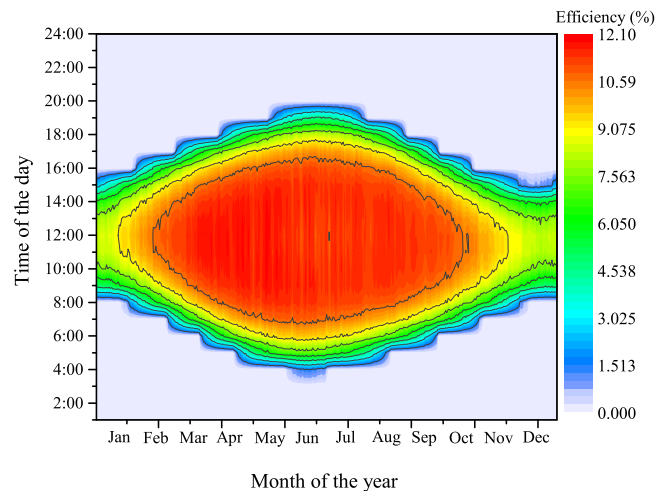


Fig. 7. Estimated SR module efficiency evaluated throughout the year 2015 as a function of the estimated irradiance and operating temperature.

the main is the noninclusion of the impact of thermal inertia on the development of the thermal profile.

From the linear regression on hourly estimated and measured temperatures for the entire year of 2015, it was concluded that the theoretical model tends to overpredict the module temperature for higher irradiance level and underpredict it for lower irradiance levels. From this, it can be inferred that the detrimental effect of temperature on the theoretical average operating efficiency would be overestimated as compared with the measured value. In other words, it is important to note that the mismatch in the predicted module temperature would result in the reduction in the theoretical overall annual energy yield used as a benchmark for comparing the operational performance.

E. Theoretical Efficiency and Energy Yield

The module efficiency depending on time-varying estimated irradiance and operating temperature is shown in Fig. 7.

In the figure, the region with a red shade represents the time zones with high operating efficiency. The lighter blue area is where irradiance has fallen to zero, and hence, the SR is not generating power. A clear dependence of efficiency on the irradiance levels can be observed from the contour lines. In fact, the contour lines resemble the solar path during the year for the installation site. Few instances of lower efficiency within the innermost contour (10:00 A.M. to 2:00 P.M. in the months of June and July) are due to high operating temperature. The maximum estimated efficiency attained by the PV module is 12.10%. The maximum predicted module dc power output is 243 W, which is achieved during maximum irradiation condition at the installation site.

The power injected into the ac grid was computed for the SR interfacing electrical system and simple control rules described in Section II. The operating power-dependent efficiency of the inverter system was modeled in accordance with the method described in [29]. The annual energy yield of the SR was theoretically estimated at 92.86 kWh/m², with an effective cumulative annual efficiency of 9.08% as seen from the ac grid. This

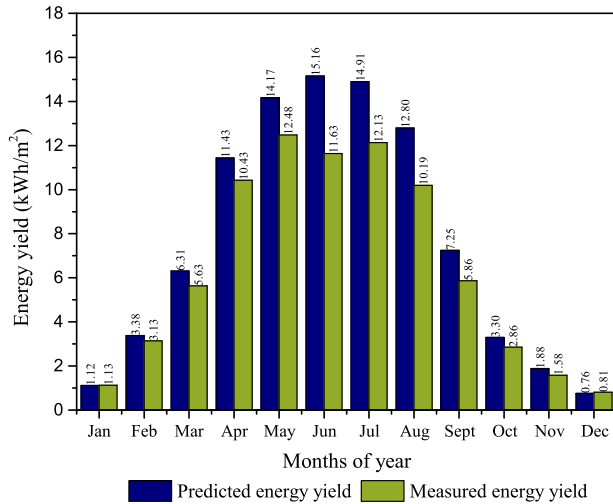


Fig. 8. Comparison between the measured energy and the predicted energy for the year 2015.

translates to an annual yield of 712 kWh/kWp, which is slightly lower than the expected range of 750–900 kWh/kWp typical for PV installations in The Netherlands. Despite this number being relatively lower than build-added PV systems (i.e., optimal tilt and orientation), it is still appealing as coming from an area with PV potential otherwise left unused.

IV. COMPARATIVE ANALYSIS WITH EXPERIMENTAL DATA

The annual energy yield measured for the year 2015 is 78 kWh/m², and the energy yield predicted from the performance model is 92.86 kWh/m², resulting in overestimation by 16%. Fig. 8 shows the monthly predicted and measured energy yield.

The measured energy yield for June is low despite the maximum irradiance received in this month. This is mostly because the SR was shut down for a week during this period. In addition, other reasons for the difference between measured and predicted energy yield are highlighted in the following.

1) *Model limitations*: Some mismatch between prediction and measurements is expected due to deviations in assumptions (material properties, shading, neglected thermal inertia, among other things), imprecise inputs such as ambient temperature and wind profile, and limited ability to represent reality through mathematical models. For instance, it was inferred in Section III-D that the mismatch in the predicted module temperature would result in the reduction in the theoretical overall annual energy yield used as a benchmark for comparing the operational performance.

2) *Error in irradiance prediction*: In calculating the energy yield, the global irradiance at the installation site based on sun's position over the site was used. When the actual on-site irradiance measurement was used, the predicted yield decreased by 2% to 91 kWh/m².

3) *Dynamic shading and shutdown*: Dynamic shading corresponding to partial coverage of SR elements due moving bikes also leads to a difference between the measured and predicted yield. It is difficult to model because of its dependence on the

TABLE I
PARAMETERS OF CONSIDERED PV MODULES [32]

Parameters	Poly-crystalline	Mono-crystalline	CIGS
Power (W)	300	345	300
Area (m ²)	2.3	1.62	2.6
V _{oc} (V)	49	69.2	69.7
I _{sc} (A)	7.4	6.39	6.4
V _{mpp} (V)	40	57.3	54.3
I _{mpp} (A)	6.75	6.02	5.5
P _{coeff} (W/°C)	-0.48	-0.38	-0.43
η _{stc} (%)	16	20	10.5

traffic behavior in terms of the number of bikes, speed of movement, and daily/seasonal patterns. Furthermore, deviation due to operational shutdowns (both scheduled and contingent) is also possible. These operational aspects have an important influence on the cumulative efficiency that must be factored in at the planning stage of the installation. As an example, the detrimental effect of dynamic shading increases with irradiance. This means that compared with the peak of the traffic pattern, the flow profile during periods of high irradiance should be considered. Such best practices are expected to standardize with the market maturity of SR technology.

4) *Individual element performance*: Comparative performance analysis based on measurements from individual modules is beyond the scope of this work due to data confidentiality. One of the best performing modules (Module number #23) had a cumulative energy yield within 5% of the predicted yield. Thus, a benchmark energy yield of 85–90 kWh/m² is a reasonable expectation.

5) *Long-term performance*: Further research is needed to ascertain the long-term performance of the SR elements with operational wear and tear, including, but not limited to, soiling. The knowledge will influence the decision on maintenance requirements of this technology.

The energy yield and the thermal profile benchmarks offered thus far are specific to PV cell technology and the installation site for the SR project. Consequently, the expected benchmarks may change if the in-module PV conversion cell is changed or the installation site is different, thus influencing the choice of inherent components of the SR technology. The subsequent section provides some insight on such considerations.

V. SOLAR ROAD AROUND THE WORLD

The extensive study detailed in Sections II–IV is further extended to examine the performance of the SR when: 1) used with different PV technologies; and 2) implemented at various locations around the world. Three main PV technologies were considered for this study, viz., polycrystalline silicon, monocrystalline silicon, and copper indium gallium and selenium (CIGS). Table I shows the module-level parameters for sample PV modules based on the above-mentioned PV technologies. Relevant datasheets can be accessed from [32].

The locations chosen for the study are Chicago (USA), Doha (Qatar), Brazzaville (Republic of Congo), Mysore (India), and Brisbane (Australia). Krommenie has been retained as a location in the study for comparative reasons. The meteorological data

TABLE II
ESH AROUND THE WORLD INCLUDING THE ANNUAL ENERGY YIELD PER
UNIT AREA FOR CONSIDERED TECHNOLOGIES

Place	ESH (kWh/m ² /day)	Annual Yield (kWh/m ²)		
		PC	MC	CIGS
Krommenie	2.84	99.2	142	64
Chicago	3.79	139	193	89
Doha	5.4	206.1	286.4	130
Brazzaville	5.85	214	312	140
Mysore	5.62	213	298	138
Brisbane	5.1	183	257	117

PC = polycrystalline, MC = monocrystalline.

for ambient temperature, wind speed, and rainfall were obtained from the “System Advisory Model” database [33] and from the National Oceanic and Administrative Association [34].

The energy yield per unit area of these different technology-based modules was evaluated based on the models and methodologies explained in Section III. That is, the same composition, optical, and thermal properties as that of the SR in Krommenie were considered for evaluating the energy yield per unit area at different chosen locations. Table II outlines both the evaluated annual energy yield per unit area and the equivalent sun hours (ESH). While the ESH is purely a measure of the insolation available at a particular place, the energy yield per unit area is a measure of both the meteorological conditions of the place as well as the PV technology performance.

As seen in Table II, the monocrystalline technology in Brazzaville performs the best out of all the technology–location combinations. It can be inferred that the PV technology with higher efficiency in a region with higher ESH exhibits a higher energy yield. However, the incident irradiance (or ESH) does not necessarily provide a complete picture when estimating a PV module’s performance. This is because the module temperature can play a vital role in determining the operational efficiency. High module temperatures can cause a significant deviation of operational efficiency from the standard testing conditions (STC)-rated efficiency, as seen in Fig. 7. Therefore, the energy yield is not the best parameter to purely evaluate the technology performance at a particular location.

To determine the impact of the diurnal variation of irradiance and the operating temperature on the performance of different PV modules, the module identity factor (MIF) is used. The MIF can be defined as the factor that indicates the proportion of the estimated PV yield actually available in the duration of interest [35]. The mathematical relation for the MIF is shown as follows [35]:

$$\text{MIF} = \frac{\text{Energy yield with varying operating efficiency} \times 100}{\text{Energy yield with constant (rated) operating efficiency}} \quad (2)$$

The greater is the value of the MIF, the lower is the reduction in performance of the technology due to the thermally induced and/or irradiance losses. That is, a MIF value of 100% indicates that the module of the given PV technology performs constantly at the STC-rated efficiency. Fig. 9 shows the variation in performance of different PV technologies at the chosen locations

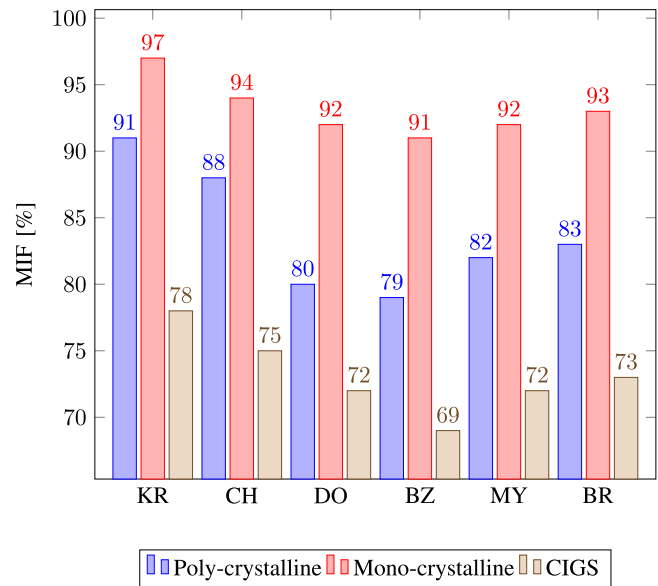


Fig. 9. Comparison of MIF values calculated for different PV technologies over various locations around the world. KR = Krommenie, CH = Chicago, DO = Doha, BZ = Brazzaville, MY = Mysore, and BR = Brisbane.

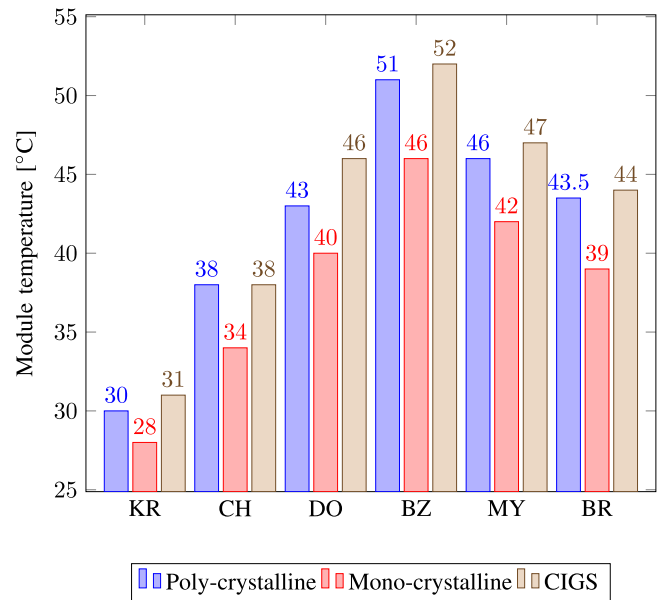


Fig. 10. Comparison of average module temperature values calculated for different PV technologies over various locations around the world. KR = Krommenie, CH = Chicago, DO = Doha, BZ = Brazzaville, MY = Mysore, and BR = Brisbane.

in terms of the MIF factor, while Fig. 10 shows the variation in the average module temperatures.

It can be observed that the CIGS module has the largest reduction in performance, even though it has a slightly better thermal coefficient as compared with polycrystalline module (see Table I). This is due to higher operating temperatures leading to lower efficiency.

The location with the highest ESH, i.e., Brazzaville, also has the least MIF value across all the considered PV technologies. This is because the higher irradiance values are also accom-

panied by the higher module temperature values experienced by the PV technologies in the location (see Fig. 10). Similarly, Kromennie, despite the enjoying the least ESH, exhibits the highest MIF value owing to the smallest average module temperature. From the considered PV technologies, monocrystalline performs the best due to the higher operating efficiency with lower sensitivity toward temperature.

Thus, it is seen that the MIF value can give insight into the thermal performance of the particular PV technology module for a given location. Additionally, it is concluded that for SR conditions, while monocrystalline silicon is the best of the three considered technologies, in terms of the thermally induced losses, Kromennie is the optimal location choice.

VI. CONCLUSION

The measured performance of the installed SR in Krommenie, near Amsterdam, is in agreement with the theoretically predicted results. The measured cumulative annual energy yield was 78 kWh/m², which is about 16% yield lower than expected (93 kWh/m²). Several factors explaining this difference were highlighted, such as model limitations, irradiance prediction error, unaccounted dynamic, and operational shutdown losses.

Based on the best performing module, which was within 5% of the predicted yield, the benchmark annual energy yield expectation for SR technology is set at 85–90 kWh/m², specific to the installation site. This number is smaller than the typical electricity yield of optimized build-added PV systems, but is appealing due to the usage of area with PV potential otherwise left unused. With market maturity, the target should be to improve this number. As compared with other roadway energy harvesting technologies, the high power and energy density potential and flexibility of energy use through grid-connected operation should be explored.

In addition, using more efficient monocrystalline cells, the annual yield can theoretically be improved by about 1.5 times for the same location as compared with polycrystalline. Cost tradeoffs are relevant, but beyond the scope of this work.

From the point of view of the MIF, Krommenie performs the best in terms of thermally induced losses. Again, the monocrystalline cell outperforms in terms of both the absolute value of the MIF and the temperature-dependent swing with high ESH locations.

For the same PV cell technology, significantly higher annual energy yields (about two times) can be obtained for locations such as Doha, Brazzaville, Mysore, and Brisbane as compared with Krommenie. CIGS cells show the highest operating temperatures, lowest MIF and the maximum temperature dependent swing in location specific MIF. Monocrystalline technology offered the highest yield at lowest operating temperatures. It is not unreasonable to expect location specific annual yields in the upwards of 150 kWh/m² with SR technology.

ACKNOWLEDGMENT

The authors would like to thank the consortium developing SolaRoad consisting of Province Noord-Holland, Strukton

Civiel West, and the Netherlands Organization for Applied Scientific Research for providing the used monitoring data, details of the construction, and a sample of the antiskid layer for analysis. SolaRoad is a joint initiative of the Province of North Holland, road construction company Strukton, electrical service company Dynniq, and the Netherlands Organisation for Applied Scientific Research. More information can be found at www.solaroad.nl.

REFERENCES

- [1] International Technology Roadmap for Photovoltaic (ITRPV), 2017. [Online]. Available: <http://www.itrpv.net/Reports/Downloads>
- [2] C. Battaglia *et al.*, "High-efficiency crystalline silicon solar cells: Status and perspectives," *Energy Environ. Sci.*, vol. 9, pp. 1552–1576, 2016.
- [3] K. Yoshikawa *et al.*, "Silicon heterojunction solar cell with interdigitated back contacts for a photoconversion efficiency over 26%," *Nature Energy*, vol. 2, 2017, Art. no. 17032, doi: [10.1038/nenergy.2017.32](https://doi.org/10.1038/nenergy.2017.32).
- [4] A. S. Dezfooli *et al.*, "Solar pavement: A new emerging technology," *Sol. Energy*, vol. 149, pp. 272–284, 2017.
- [5] R. Pool, "Sunshine highways," *Eng. Technol.*, vol. 6, no. 2, pp. 54–57, Mar. 2011.
- [6] M. S. Wu *et al.*, "Economic feasibility of solar-powered led roadway lighting," *Renew. Energy*, vol. 34, no. 8, pp. 1934–1938, 2009.
- [7] Z. Rajab *et al.*, "Economic feasibility of solar powered street lighting system in Libya," *Proc. 8th Int. Renew. Energy Congr.*, Amman, Jordan, 2017, pp. 1–6.
- [8] A. Shekhar *et al.*, "Grid capacity and efficiency enhancement by operating medium voltage AC cables as DC links with modular multilevel converters," in *Proc. Int. J. Electr. Power Energy Syst.*, 2017, vol. 93, pp. 479–493.
- [9] V. Prasanth *et al.*, "Green energy based inductive self-healing highways of the future," in *Proc. IEEE Transp. Electrific. Conf. Expo.*, Dearborn, MI, USA, 2016, pp. 1–8.
- [10] P. Venugopal *et al.*, "Roadway to self-healing highways with integrated wireless electric vehicle charging and sustainable energy harvesting technologies," *Appl. Energy*, vol. 212, pp. 1226–1239, 2018.
- [11] B. Holdsworth, "Solar energised roads and infrastructures," *Refocus*, vol. 4, no. 3, pp. 58–60, 2003. [Online]. Available: [https://doi.org/10.1016/S1471-0846\(03\)80123-3](https://doi.org/10.1016/S1471-0846(03)80123-3)
- [12] R. B. Mallick *et al.*, "Altimetric original articles harvesting energy from asphalt pavements and reducing the heat island effect," *Int. J. Sustain. Eng.*, vol. 2, no. 3, pp. 214–228, 2009.
- [13] D. S. N. M. Nasir *et al.*, "Influence of urban form on the performance of road pavement solar collector system: Symmetrical and asymmetrical heights," *Energy Convers. Manage.*, vol. 149, pp. 904–917, 2017.
- [14] H. Roshani *et al.*, "Energy harvesting from asphalt pavement roadways vehicle-induced stresses: A feasibility study," *Appl. Energy*, vol. 182, pp. 210–218, 2016.
- [15] C. H. Yang *et al.*, "Development of impact-based piezoelectric road energy harvester for practical application," in *Proc. IEEE Int. Conf. Renew. Energy Res. Appl.*, Birmingham, U.K., 2016, pp. 375–378.
- [16] J. Rivas *et al.*, "Road vibrations as a source to detect the presence and speed of vehicles," *IEEE Sens. J.*, vol. 17, no. 2, pp. 377–385, Jan. 15, 2017.
- [17] R. Abinaya *et al.*, "An intelligent street light system based on piezoelectric sensor networks," in *Proc. 4th Int. Conf. Electron. Commun. Syst.*, Coimbatore, India, 2017, pp. 138–142.
- [18] T. Celik *et al.*, "Solar-powered automated road surveillance system for speed violation detection," *IEEE Trans. Ind. Electron.*, vol. 57, no. 9, pp. 3216–3227, Sep. 2010.
- [19] B. Diong, "Justification and conceptual design of solar-powered traffic signal systems," in *Proc. Int. Conf. Renew. Energy Res. Appl.*, Milwaukee, WI, USA, 2014, pp. 595–600.
- [20] D. C. Vageesh *et al.*, "Joint placement and sleep scheduling of grid-connected solar powered road side units in vehicular networks," in *Proc. 12th Int. Symp. Model. Optim. Mobile, Ad Hoc, Wireless Netw.*, Hammamet, Tunisia, 2014, pp. 534–540.
- [21] Q. I. Ali, "Event driven duty cycling: An efficient power management scheme for a solar-energy harvested road side unit," *IET Elect. Syst. Transp.*, vol. 6, no. 3, pp. 222–235, Sep. 2016.
- [22] M. B. Naik *et al.*, "Small-scale solar plants coupled with smart public transport system and its coordination with the grid," *IET Elect. Syst. Transp.*, vol. 7, no. 2, pp. 135–144, Jun. 2017.

- [23] “Welcome to the world’s first solar road [News Briefing],” *Eng. Technol.*, vol. 12, no. 1, p. 10, Feb. 2017.
- [24] B. Xiang *et al.*, “A novel hybrid energy system combined with solar-road and soil-regenerator: Dynamic model and operational performance,” *Energy Convers. Manage.*, vol. 156, pp. 376–387, 2018.
- [25] Nov. 2017. [Online]. Available: www.solaroad.nl
- [26] C. Rigollier *et al.*, “On the clear sky model of the 4th European Solar Radiation Atlas with respect to the Heliosat method,” *Sol. Energy*, vol. 68, no. 1, pp. 33–48, 2000.
- [27] A. Shekhar *et al.*, “Solar road operating efficiency and energy yield—An integrated approach towards inductive power transfer,” in *Proc. Eur. Photovoltaic Sol. Energy Conf.*, Hamburg, Germany, 2015, pp. 2622–2627.
- [28] T. M. Klucher, “Evaluation of models to predict insolation on tilted surfaces,” *Sol. Energy*, vol. 23, no. 2, pp. 111–114, 1979.
- [29] A. H. M. Smets *et al.*, *Solar Energy: Fundamentals, Technology and Systems*. Cambridge, U.K.: UIT Cambridge, 2015, pp. 225–339.
- [30] M. K. Fuentes, “A simplified thermal model for flat-plate photovoltaic arrays,” Sandia Nat. Lab., Albuquerque, NM, USA, Tech. Rep. SAND85-0330, 1987.
- [31] K. Jager *et al.*, “Angular resolved scattering measurement of nanotechnology of nanotexture substrate,” *Meas. Sci. Technol.*, vol. 22, 2011, Art. no. 105601.
- [32] Datasheets for Sunpower Solar Panels, Nov. 2017. [Online]. Available: www.zonnepanelen.net
- [33] System Advisor Model, Nov. 2017. [Online]. Available: <https://sam.nrel.gov>
- [34] National Center for Environmental and Information, National Oceanic and Atmospheric Administration, U.S. Dept. Commerce, Nov. 2017. [Online]. Available: <http://www.ncdc.noaa.gov>
- [35] N. S. Narayan, *Dutch Photovoltaic Energy Portal*, Delft University of Technology, Delft, The Netherlands, 2014, p. 63.



Aditya Shekhar received the M.Sc. (*cum laude*) degree in electrical power engineering from the Delft University of Technology, Delft, The Netherlands, in 2015, where he is currently working toward the Ph.D. degree in dc systems.

He received an honors for his internship at the Netherlands Organisation for Applied Scientific Research (TNO) in 2014. His work with TNO on solar roads was chosen for the plenary presentation in the 31st European Photovoltaic Solar Energy Conference and Exhibition, Hamburg, Germany, 2015. His research interests include the development of energy technologies aiming toward a sustainable future.



Vinod Kumar Kumaravel received the master’s degree in sustainable energy technology (with specialization in photovoltaic devices and systems) from the Delft University of Technology, Delft, The Netherlands, in 2016.

He is currently a Remote Solar Designer with Sungevity International, Amsterdam, The Netherlands.



Stan Klerks received the M.Sc. degree in architectural design and engineering from the Eindhoven University of Technology, Eindhoven, The Netherlands, in 2006.

He joined the Netherlands Organisation for Applied Scientific Research, The Hague, The Netherlands, as a Researcher in the field of sustainability of the built environment in 2008. In 2011, he joined the SolaRoad team as a System Architect. In this role, he led the multidisciplinary design team and was responsible for the different SolaRoad system designs for the first public road equipped with photovoltaic technology, installed in the Netherlands in 2014.



Sten de Wit received the Ph.D. degree in thermal modeling of buildings from the Delft University of Technology, Delft, The Netherlands, in 2001.

He is a Senior Scientist with the Netherlands Organisation for Applied Scientific Research (TNO), The Hague, The Netherlands. Since 2010, at TNO, he has been the driving force in the research on the integration of solar technology in road infrastructure. His current research interests include the interface of infrastructure, energy, and mobility, focusing on cutting CO₂ emissions and boosting sustainable energy production.



Prasanth Venugopal received the B.Tech. degree (silver medal) in electrical and electronics engineering from Amrita Vishwa Vidyapeetham, Coimbatore, India, in 2010, and the M.Sc. (*cum laude*) degree in electrical engineering from the Delft University of Technology, Delft, The Netherlands, in 2012, where he continued his Ph.D. research in dynamic inductive power transfer.

He is currently a Senior Electrical Engineer with Qualcomm Halo, Munich, Germany, working on applying electromagnetic field theory to the areas of power electronics and its control.



Nishant Narayan received the M.Sc. degree in sustainable energy technology (specializing in photovoltaic systems) from the Delft University of Technology, Delft, The Netherlands, in 2013, where he is working toward the Ph.D. degree in developing modular solar home systems and off-grid solutions for improving energy access in low-resource contexts.



Pavol Bauer received the master’s degree in electrical engineering from the Technical University of Košice, Košice, Slovakia, in 1985, and the Ph.D. degree in dynamic analysis of ac power converters from the Delft University of Technology, Delft, Netherlands, in 1995.

Since 2016, he has been a Full Professor with the Department of Electrical Sustainable Energy, Delft University of Technology, where he is the Head of the DC Systems, Energy Conversion and Storage Group. He has worked on many projects in collaboration with industries for developing smart cities with photovoltaic charging of electric vehicles, photovoltaic storage integration, and contactless charging.



Olindo Isabella received the Ph.D. (*cum laude*) degree in light management in thin-film silicon solar cells from the Delft University of Technology, Delft, The Netherlands, in 2013.

Between 2011 and 2012, he was a Visiting Researcher with the National Institute of Advanced Industrial Science and Technology, Tsukuba, Japan, where he worked on high-performance thin-film a-SiGe:H absorbers for multijunction applications. He is currently an Associate Professor in the Photovoltaic Materials and Devices Group, Delft University of

Technology, where he supervises optoelectrical device modeling activities, novel concepts of light management, the development of high-efficiency solar cells based on crystalline silicon and thin-film silicon technologies, and advanced power modeling for custom photovoltaic systems.



Miro Zeman received the Ph.D. (*cum laude*) degree in amorphous silicon from the Slovak University of Technology, Bratislava, Slovakia, in 1989.

In 2009, he became a Full Professor with the Delft University of Technology, Delft, The Netherlands, where he leads the Photovoltaic Materials and Devices Group and is the Head of the Electrical Sustainable Energy Department. He is a leading expert in light management, modeling, and development and application of novel materials and nanostructures in silicon-based solar cells.